[2] M. Fukuda, A. Hasegawa, T. Tanno, et al., J. Nucl. Mater., 442(2013)S273.
[3] R. W. Siegel, S. M. Chang, R.W. Balluffi, Acta Metall., 28(1980)249.
[4] W. Z. Han, M. J. Demkowiczand, E.G. Fu, et al., Acta Materialia, 60(2012)6341.
[5] B. K. Basu, C. Elbaum, Acta Metall., 13(1965)1117.
[6] M. J. Demkowicz, O. Anderoglu, X. Zhang, et al., J. Mater. Res., 26 (2011)1666.
[7] H. Grimmer, Acta Crystallogr, Sect. A, 32(1976)783.
[8] R. J. Kurtz, H. L. Heinisch, J. Nucl. Mater., 329-333(2004)1199.

4 - 10 First-principles Investigation of Vacancy and Self-interstitial Atom Formation Energy at Grain Boundary in Tungsten

He Wenhao, Gao Xing and Wang Zhiguang

Materials served in nuclear energy systems usually expose to high irradiation doses of particles. Projectile particles lead to creations of a large numbers of vacancies (Vs) and self-interstitial atoms (SIAs) in materials. The SIAs may gather to form dislocation loops and stacking-fault tetrahedrons, and the Vs usually gather to form voids. These defects contribute to material swelling, hardening, amorphization and embrittlement, and may accelerate material failure under irradiation[1]. Extensive experimental results demonstrated that nano-crystalline materials generally showed good radiation resistance than common poly-crystalline materials because there existed a high fraction of grain boundaries (GBs) in nano-crystalline materials[2]. However, threshold stresses in Nabarro–Herring creep provided the earliest indication that point defects sink strengths might depend on GB structures[3]. Usually, GBs that have atomic configurations such that both the ability to trap intrinsic point defects and Frenkel pair annihilation rates are high will be good sinks for Vs and SIAs. Here, we mainly study the atomic configurations around GBs effects on the ability to trap Vs and SIAs. Tungsten is one of the promising candidates for plasma facing materials (PFMs), such as the first wall materials and divertor of magnetic confinement fusion reactor due to its high melting temperature, high thermal conductivity and low sputtering erosion. In this study, the abilities to trap Vs and SIAs of eight symmetric tilt GBs in tungsten are investigated through first-principles calculations. These GBs are constructed by the coincidence site lattice model[4].

First-principles total energy calculations were carried out with the Vienna Ab initio Simulation Package (VASP) based on the density functional theory (DFT). The projected augmented wave (PAW) pseudopotentials were employed in the calculations within the generalized gradient approximation (GGA) with Perdew and Wang functional for the exchange and correlation energies. A cutoff energy of 400 eV was used for the plane-wave expansion. The internal structural relaxations stopped when the residual force on each atom was less than 0.01 eV/Å. Both atomic positions and volumes of supercells were allowed to relax in all calculations.

The vacancy formation energy $E_{\mathrm{V}}^{\mathrm{f}}$ at each site around GBs (bulk) can be calculated by,

$$E_{\mathrm{V}}^{\mathrm{f}} = E_{(\mathrm{GB(bulk),V})} - E_{(\mathrm{GB(bulk)})} + e_{\mathrm{W}}, \tag{1}$$

where $E_{(\mathrm{GB(bulk),V})}$ is the total energy of the supercell containing a vacancy around the GB (bulk), $E_{(\mathrm{GB(bulk)})}$ is the total energy of the supercell containing the clean GB (bulk), and e_{W} is the energy of a tungsten atom in bulk environment.

The SIA formation energy $E_{\mathrm{SIA}}^{\mathrm{f}}$ in each interstitial site at GBs (bulk) can be calculated by,

$$E_{\mathrm{SIA}}^{\mathrm{f}} = E_{(\mathrm{GB(bulk),SIA})} - E_{\mathrm{GB(bulk)}} - e_{\mathrm{W}}, \tag{2}$$

where $E_{(\mathrm{GB(bulk),SIA})}$ is the total energy of the supercell containing a SIA in the interstitial site at a GB (bulk).

$E_{\mathrm{V}}^{\mathrm{f}}$ versus hard-sphere radius r_0 of the vacancy is shown in Fig. 1(a). In this study, the r_0 is defined as the largest hard-sphere radius which can be inserted into the vacancy. The hard-sphere radius of tungsten atom is defined as half the distance between the nearest neighbors in bcc tungsten, which is 1.38 Å in equilibrium bcc tungsten. As shown in Fig. 1(a), the $E_{\mathrm{V}}^{\mathrm{f}}$ rapidly increases as r_0 increases and reaches its largest value as the r_0 is 1.38 Å. Then the $E_{\mathrm{V}}^{\mathrm{f}}$ slowly decreases as the r_0 keeps increasing. This result is reasonably sound since the binding energy in bcc tungsten is the largest when the first nearest neighbor distance is 2.76 Å. Any shorter/longer distance between them will induce the decrease of the binding energy thus make the formation of a vacancy easier. The r_0 can refer to the atom density around GB. The smaller the r_0 is, the larger the atomic density is. According to the relation between $E_{\mathrm{V}}^{\mathrm{f}}$ and r_0, it is easily found that any denser/looser atomic configuration around GB than that in

bulk is helpful to form vacancy, that is, the ability of the GB to trap Vs is stronger. The relationship between the SIA formation energy $E^{\mathrm{f}}_{\mathrm{SIA}}$ around GBs and the hard-sphere radius r_0 of the interstitial site is showed in Fig. 1(b). As with the hard-sphere radius defined for vacancy, r_0 is defined as the largest hard-sphere radius which can be added into the interstitial site. The formation energy $E^{\mathrm{f}}_{\mathrm{SIA}}$ of SIA at GBs decreases as the hard-sphere radius r_0 of the interstitial sites increases. According to the relationship between $E^{\mathrm{f}}_{\mathrm{SIA}}$ and r_0, it is easily found that the larger interstitial site at GBs is more helpful to form SIA, that is, GBs containing larger interstitial sites have stronger ability to trap SIAs.

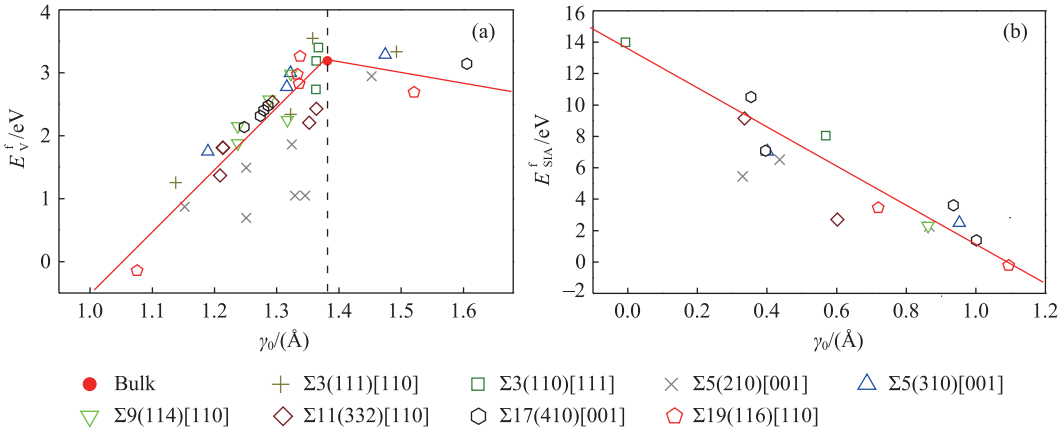

Fig. 1 (color online) (a) Vacancy formation energy $E^{\mathrm{f}}_{\mathrm{V}}$ vs. the hard-sphere radius r_0 of the vacancy. The black vertical dash line refers to the hard-sphere radius 1.38 Å of the vacancy in bulk. (b) The SIA formation energy $E^{\mathrm{f}}_{\mathrm{SIA}}$ vs. hard-sphere radius r_0 of the interstitial sites. The red solid line is drawn to guide the eyes.

References

[1] K. E. Sickafus, R. W. Grimes, J. A. Valdez, et al., Nat. Mater., 2(2007)217.
[2] H. Kurishita, Y. Amano, S. Kobayashi, et al., J. Nucl. Mater., 367(2007)1453.
[3] M. F. Ashby, Scr. Metall, 3(1969)837.
[4] H. Grimmer, Acta Crystallogr. Sect. A, 32(1976)783.

4 - 11 Irradiation Damage of Ti_3AlC_2: Damage Evolution and Structure Transformation

Deng Tianyu, Sun Jianrong, Wang Zhiguang, Pang Lilong, Li Binsheng, Shen Tielong, Zhu Yabin, Cui Minghuan, Tai Pengfei and He Wenhao

Ceramics compound Ti_3AlC_2 exhibits nano-layered structure and has the properties of both ceramic and metal. It includes easy machinability, good high-temperature resistance and irradiation–damage tolerance. So it's supposed to be a candidate for future nuclear reactor. For example, it can be used as a coatings on Zr cladding materials. It can withstand severer irradiation damage and prevent the reaction between water and Zr. Therefore the understanding of Ti_3AlC_2under irradiation is fundamentally important for the development of nuclear materials[1].

Ion irradiations were carried out with 1 MeV C^{4+} ions at room temperature in a terminal of 320 kV research platform. The doses were 1×10^{15}, 5×10^{15}, 1×10^{16}, 5×10^{16}, 1×10^{17}ions/cm^2, respectively. In Fig. 1, we calculated the DPA and ion concentration profile with the help of SRIM 2008.

From the XRD patterns of Ti_3AlC_2 shown in Fig. 2 where samples irradiated among different doses at room temperature, all the samples exhibit crystalline and there is no evidence of amorphization. A decrease and strong broadening of all peaks could be found for all irradiated samples, especially for peaks of (101), (004) and (106), which indicated the structural distortion induced by irradiation. However, some specific peaks intensity has strengthened and even new peaks emerge at 35.1, 36.5, 44.0, 58.5 and 62.5. These peaks may derive from phase transitions from αTi_3AlC_2 to βTi_3AlC_2. The bond between Al atoms and surrounding Ti or C atoms is relatively weak, so the shear stress induced by irradiation will push the Al layer and form the new phase[2].